Journal of Computational Acoustics, Vol. 3, No. 3 (1995) 203–218

TEMPORAL CHARACTERISTICS OF ACOUSTIC RAY PROPAGATION THROUGH "INFINITE" AND "BOX MODEL" TURBULENCE

MICHAEL KARWEIT
Department of Chemical Engineering,
Johns Hopkins University, Baltimore, MD, 21218

PHILIPPE BLANC-BENON*
Laboratoire Mécanique des Fluides et Acoustique, URA CNRS 263
Ecole Centrale de Lyon, BP 163-69131 ECULLY Cedex, France

Received 15 September 1994
Revised 24 March 1995

In this work, we investigate the temporal characteristics of acoustic ray propagation through simulated, weakly turbulent temperature fields. In a first set of experiments, we generate ensembles of random scalar fields from randomly oriented Fourier temperature modes. Then, by integrating the ray trace equations, we estimate the distribution of arrival times for rays propagating a distance R through them. We demonstrate that these arrival time distributions are Gaussian for both axial and 3-D propagation and are primarily determined by the lower wave numbers of the 1-D fluctuation spectrum.

In a second set of experiments, we generate random fields comprised of Fourier modes prescribed on a lattice, as in "box model" turbulence. In these simulations, we find that acoustic travel times are significantly affected both by the periodicity of the fields and by the direction of acoustic propagation with respect to the orientation of the box. Both effects can ultimately be attributable to an inadequate representation of the low wave number region of the 1-D spectrum. We suggest that these artifacts of simulated periodic fields may preclude their use for acoustic propagation studies.

1. Introduction

The phase, frequency and amplitude distortion of acoustic and optical waves propagating through turbulence (random inhomogeneous media) have an important impact on a wide range of signals: radio transmission, optical images, sonar. Consequently, one would like to know the pdf (probability density function) of the scattering of the signal as a function of the statistical characteristics of the inhomogeneities of the medium. But, since obtaining a full analytic result would seem not to be possible, researchers have focused on the more modest goal of trying to predict some of the lower moments of the pdf for media which are only weakly inhomogeneous.[1–4] In those cases where the media have only temperature

*This work was carried out while the second author was a visiting scholar at Johns Hopkins University.

(scalar) inhomogeneities, phase screen approaches and the parabolic approximation have provided important results on scattering.[5,6]

In this paper, we focus on the problem by numerically following acoustic waves through simulated "turbulence". For weakly inhomogeneous media when the acoustic frequencies are high and the geometric approximation is valid, trajectories of acoustic (optic) phase points can be followed via the ray-trace equations. If these phase points are followed out to, say, a distance R over an ensemble of statistically-similar simulated fields, one can accumulate the distribution of travel times $t(R)$ and infer its pdf. Then, depending on further assumptions, these travel time variations can be related to phase and frequency distortion of either acoustic or optical signals.

Karweit *et al.*[7] used the above method to estimate acoustic travel-time variance in inhomogeneous velocity fields. In that work, he also introduced a method of producing "cheap turbulence" which could be used for carrying out numerical experiments in acoustic propagation. (See also Blanc-Benon, *et al.*[8] for further discussion on the numerical scheme.) Previous works, e.g., Refs. 1–6, have characterized the statistical behavior of acoustic dispersion in terms of the following ensemble properties of the propagating media: the mean and mean-square values of the fluctuations and their spatial derivatives, the inner and outer length scales of the fluctuation field, and the fluctuation spectrum. Recognizing that these field properties could be obtained without underlying dynamics, Karweit constructed random velocity fields whose spectra and one- and two-point correlations matched those of experimental turbulence data. Insofar as these fields were composed of sums of non-integrally-related random Fourier modes, the fields were essentially infinite in extent. And although individual fields did not have the properties of a dynamically-determined process, the ensemble of fields possessed those characteristics relevant to acoustic dispersion. The role of dynamics is further obviated because acoustic propagation is much faster than any scale of turbulent motion. Consequently, in most propagation simulations a "frozen field" approximation may be used.

This idea was later used by Juvé *et al.*[9] and Karweit and Blanc-Benon[10] for propagation through temperature fields.

In this paper, we use the same approach to address two questions. The first is an acoustic one: What is the pdf of arrival-time scattering for acoustic rays propagating through fields of temperature inhomogeneities? Here we obtain an empirical result.

The second is a modeling question: What characteristics must exist in simulated inhomogeneous fields, if they are to be used in numerical experiments involving acoustic-propagation?

In principle, one would like to produce an ensemble of simulated turbulent fields whose spatial and temporal characteristics are governed by the Navier–Stokes equations. Turbulence researchers have essentially achieved this, having developed not only sophisticated approximate models, but also complete numerical solutions of evolving fields. These schemes, however, being based on a regular lattice of Fourier modes, produce fields which have restricted length scales and finite size, i.e., "box turbulence". But they do contain proper dynamics, and they can be spatially-extended through their inherent periodicity. The

question is, could such fields be effectively used in simulations of long-distance acoustic propagation, say, farther than one periodic length? In this paper, we address this question and demonstrate that using such fields may lead to significant problems within even one period.

2. The Simulation of Fields based on Fourier Modes

In our investigation of acoustic dispersion through scalar-inhomogeneous fields, we will use two slightly different versions of Karweit *et al.*[7] for constructing the simulated fields–both involving a sum of Fourier modes. The first, which we will henceforth refer to as the "random model", is based on fields which are constructed from non-integrally-related random Fourier modes. The second, identified as the "box model", is based on fields constructed from a regularly-spaced lattice of Fourier modes. This latter scheme produces integrally-related Fourier wave vectors and periodic fields. See, for example, Rogallo[11] for the construction of traditional box-model turbulence.

In each case random, isotropic, scalar (temperature) fields are prescribed as:

$$T'(\mathbf{x}) = \sum_{j=1}^{N} A^{[j]}(k^{[j]}) \exp(i\mathbf{k}^{[j]} \cdot \mathbf{x}),$$

where N is the number of modes comprising the field, $A(k)$ is the complex amplitude coefficient determined by the chosen temperature-fluctuation spectrum, and $k^{[j]}$ is the wave number corresponding to the jth Fourier wave vector $\mathbf{k}^{[j]}$.

In our random model experiments, each field is composed of 2000 Fourier modes whose wave numbers are equally spaced between 1 m^{-1} and 60 m^{-1}. The directions of the corresponding wave vectors are selected randomly over the surface of the sphere in k-space to ensure statistically-isotropic fluctuation fields. See Fig. 1(a) for a 2-D illustration.

In our box model experiments, each field is composed of 2744 Fourier modes corresponding to wave vectors defined on a $14 \times 14 \times 14$ 3-D lattice, where the wave vector spacing dk_i on the lattice in each of the three directions i is $dk_i = 1/(3l_0)$. l_0 is a length scale of the temperature spectrum and will be defined below. This lattice, then, prescribes wave vector components as $k_i = ndk_i$, where n takes integer values independently in each direction from -7 to 6. (Figure 1(b) illustrates the distribution of these wave vectors.) The resulting field has a spatial period of $2\pi/dk_i = 6\pi l_0$. (The unusually sized lattice $14 \times 14 \times 14$ was chosen so that the number of independent modes in both the random and box model were roughly equivalent.)

For both models, the phases of the wave vectors are randomly chosen over $0 - 2\pi$ by selecting the real and imaginary parts of their complex coefficients $A(k)$, where the absolute value of each coefficient $|A(k)|$ is specified in accordance with a prescribed temperature spectrum.

We note that, since we want to produce real fields, i.e., fields with no imaginary components, for every Fourier mode $A(k)\exp(i\mathbf{k} \cdot \mathbf{x})$ with an imaginary component there must exist a conjugate mode $A^*(k)\exp(-i\mathbf{k} \cdot \mathbf{x})$. In the random model, of the 2000 modes, only

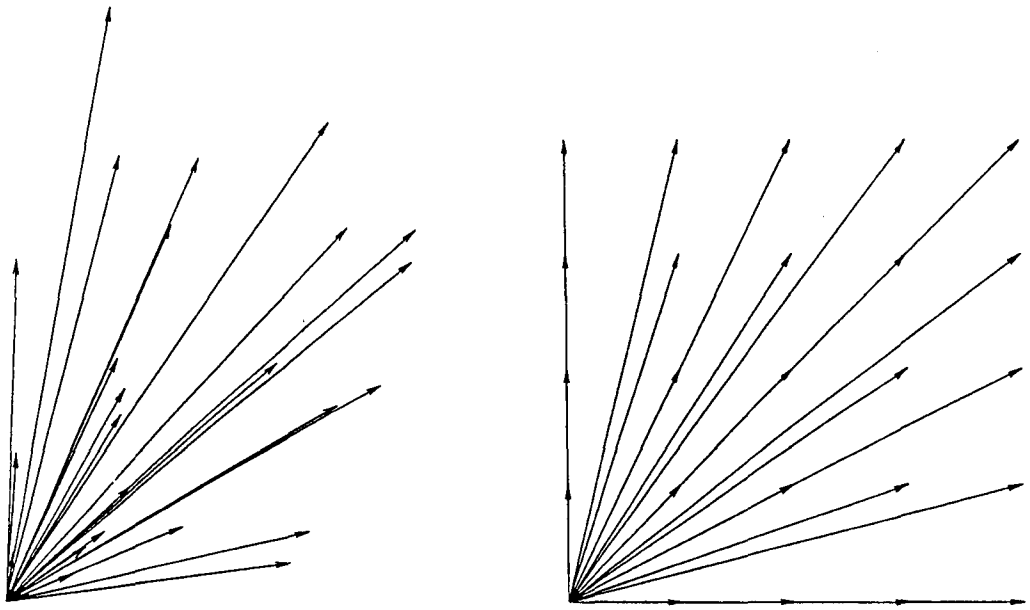

Fig. 1. Distributions of wave vectors for a random model (a) and a box model (b) field. For simplicity, the figures illustrate typical wave vector distributions in one quadrant of a 2-D field.

half (1000) are independent. In the box model, of the 2744 modes, more than half (1646) are independent. This difference is due to the fact that a number of wave vectors defined on the lattice—those at the Nyquist frequency—have no conjugate counterparts.

In all the present experiments we choose a Gaussian-derived fluctuation spectrum. Although not representative of true turbulence, this spectrum is often used as a practical simplification. The advantage is that one can explicitly calculate the relationship between the fluctuation power spectrum and the two-point spatial correlation. We begin by prescribing a Gaussian two-point temperature spatial correlation function:

$$C(r) = \frac{\langle T'(\mathbf{x}+\mathbf{r})T'(\mathbf{x})\rangle}{\langle T'(\mathbf{x})^2\rangle} = \exp(-r^2/l_0^2)\,,$$

where r is the spatial separation and l_0 is the single length scale that defines the characteristic scale of inhomogeneities of the field. For such a function, the integral length scale of the inhomogeneities is $L_f = \sqrt{\pi} l_0/2$. For the present work we have taken $l_0 = 0.1$ m.

Then, by taking the Fourier transform of this correlation function, we obtain the 3-D power spectrum:

$$G(k) = \frac{\theta^2 k^2 l_0^3}{2\sqrt{\pi}} \exp\left(-k^2 l_0^2/4\right)$$

(Ref. 12). θ^2 is mean square temperature fluctuation of the field. For a wave vector of length k, the amplitude of the temperature fluctuation associated with that mode is

$|A(k)| = \sqrt{G(k)\Delta k}$, where Δk is the distance in wave number to the next Fourier mode. For the random model, Δk is constant since the wave vectors comprising the field are selected with equal spacing in k. For the box model, however, the situation is more complicated. Not only are the wave numbers associated with the latticed wave vectors nonuniformly distributed in k, there are also groups of wave vectors having the same value of k, and the spectral amplitude must be partitioned amongst them.

Summing the contributions over N wave vectors yields one realization of a fluctuating, isotropic temperature field whose integral length scale is L_f. In ensemble, these fields have an expected value of $\langle T'(\mathbf{x})\rangle = 0$, and a mean-square fluctuation of $\langle T'(\mathbf{x})^2\rangle = \theta^2$. Our experiments use $\sqrt{\theta^2} = 3.53°\text{C}$.

3. Propagation of Acoustic Waves

For each of our two models, we consider acoustic propagation in which the geometric approximation is valid, and for which the ray-trace equations describe the propagation of phase points on an acoustic wavefront. (See Neubert and Lumley[13] and Candel[14] for detailed derivations of the conditions.) Each perturbation field is considered "frozen" and is individually constructed from Fourier modes as described above.

For acoustic propagation, each temperature fluctuation field is a perturbation field $\epsilon(\mathbf{x}) = T'(\mathbf{x})/T_0$, which can then be interpreted as an acoustic celerity field $c(\mathbf{x}) = c_0\sqrt{(1+\epsilon(\mathbf{x}))}$, where c_0 is the unperturbed sound speed of 340 m/s at the reference temperature $T_0 = 293°\text{C}$. It is the celerity field on which the following ray-trace equations[15] are based:

$$\frac{dx_i}{dt} = c^2(\mathbf{x})s_i\,,$$

$$\frac{ds_i}{dt} = -\frac{1}{c(\mathbf{x})}\frac{\partial c(\mathbf{x})}{\partial x_i}\,.$$

$\mathbf{s}$ is an auxiliary "slowness" vector defined as $\mathbf{s} = \mathbf{n}/c$, with $\mathbf{n}$, the unit vector normal to the acoustic wavefront. In all our simulations, we begin at $\mathbf{x} = 0$ with an acoustic phase point having an initially prescribed direction of propagation—the x_1 direction. Numerical integration is carried out using a fourth order Runge–Kutta scheme with a time step $\Delta t = 1/(c_0 k_{\max})$, where $k_{\max}$ is the magnitude of the largest wave vector comprising the field. This choice of Δt is detailed in Blanc-Benon *et al.*[8]

To build a pdf of acoustic arrival times, over a large ensemble of statistically-similar perturbation fields, we numerically integrate the ray-trace equations and follow the trajectory of one phase point to a radial distance R from its initial position. The distribution of times becomes our empirical estimate of the pdf.

4. Experiments Using the Random Model

Using the random model, we carry out two sets of propagation experiments: one governed by the complete set of ray-trace equations, the other governed by a restricted set in which the phase point is allowed to propagate only along its initial direction (axial propagation).

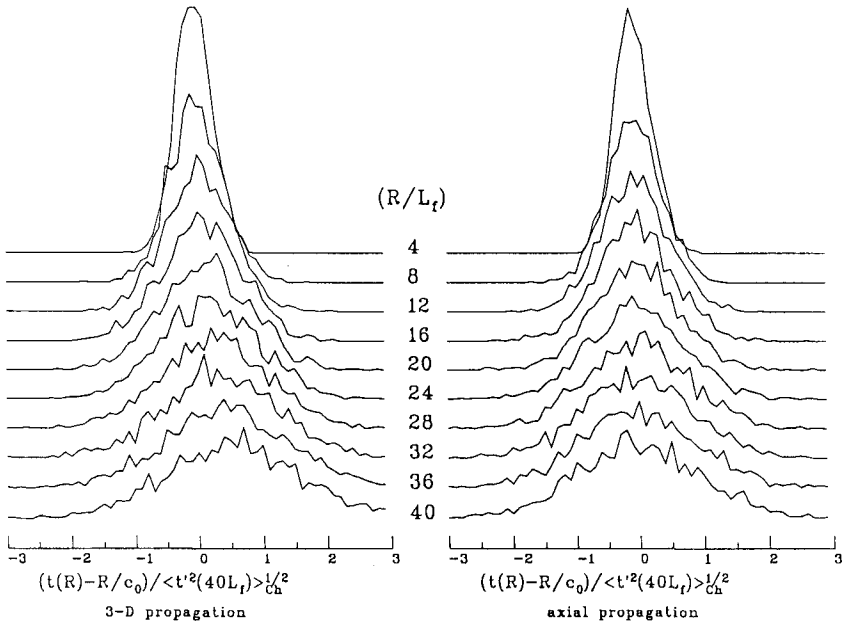

Fig. 2. Distribution of arrival times of acoustic rays $t(R)$ as a function of travel distance R for 3-D and axial propagation. Distributions are normalized with respect to the reference time R/c_0 and the Chernov prediction of arrival-time variance at a distance of $40L_f$ $\langle t'^2(40L_f)\rangle_{Ch}$.

This latter set of experiments simulates an approximation due to Chernov[1] who used the restriction to estimate the variance of acoustic arrival times in inhomogeneous media.

To follow the trajectory of an acoustic phase point determined by the Chernov assumption, we remove all effects of nonaxial influence. This reduces the number of ray-trace equations from six to two.

Distributions of arrival times of phase points traveling through temperature fields under these two sets of governing equations are given in Fig. 2. The distributions are normalized with respect to a mean arrival time of R/c_0, i.e., an unperturbed acoustic ray; and with respect to the arrival time variance at $R = 40L_f$ as estimated by Chernov.[1]

In principle, we can make valid inferences about arrival time distributions over the entire distance of $R = 40L_f$. However, if we want to make the assumption that time variation may be equated to phase variation, then our results would be valid to only about half that distance because of the potential occurrence of caustics. The connection between time variation and acoustic phase becomes unclear after a caustic. Our estimate for the range of validity comes from the theoretical analysis of White[16] and the numerical experiments of Blanc-Benon *et al.*[17] These works show that first caustics occur at distances of order $(\sqrt{\epsilon^2})^{-2/3}L_f$. In the present study, that distance is approximately $R = 21L_f$.

5. Lower Order Moments

Mean travel times are nominally R/c_0. However, as evident in Fig. 2, there is a systematic lengthening of travel time beyond R/c_0 as R increases in the 3-D case. These increases

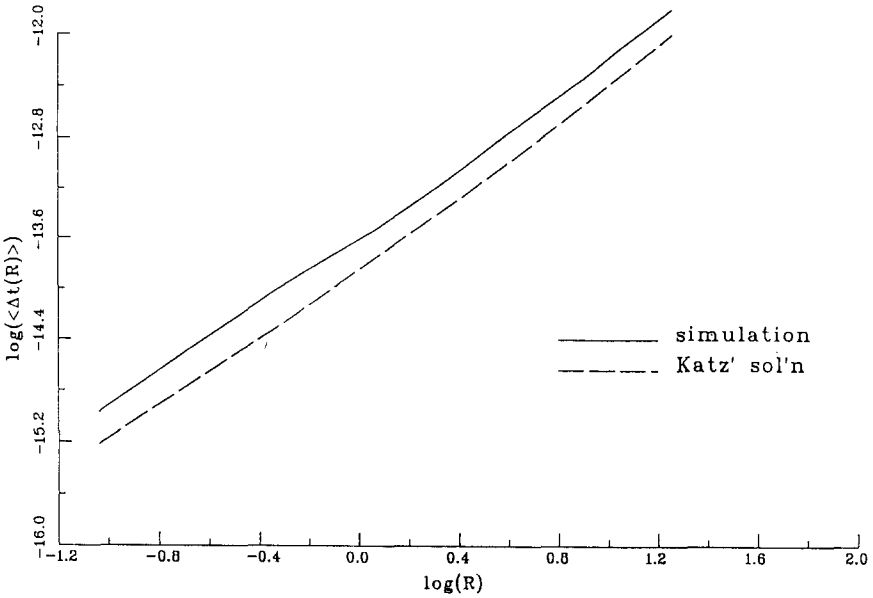

Fig. 3. Comparison of average retardation times $\langle \Delta t(R) \rangle$ between the 3-D simulations and the 2-D Katz estimate as a function of distance of propagation R. Logarithms are plotted to show functional similarity.

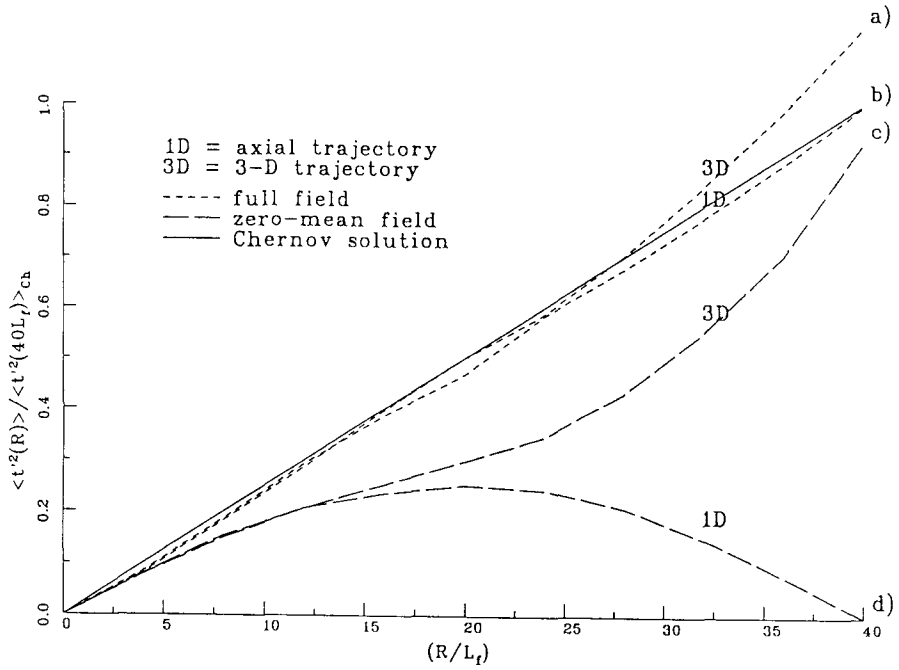

Fig. 4. Arrival-time variance $\langle t'^2(R) \rangle$ of acoustic rays as a function of propagation distance R for both axial and 3-D propagation. Curves are presented for simulations with and without the mean fields removed. Results are accumulated over 2000 realizations and normalized with respect to the Chernov solution $\langle t'(R)^2 \rangle_{Ch}$ at a distance of $R = 40L_f$. The Chernov solution is plotted for comparison.

have been predicted by Katz[4] in a 1- and 2-D analysis relating travel distance with time, i.e., $R(t)$. The increase consists of two parts: (1) the increase of travel time associated with a phase point spending more time in regions of low celerity than in high celerity, and (2) for 2-D propagation, an increase associated with the meandering of the phase point and, consequently, the longer path to reach a distance R.

If we invert the Katz result to obtain an average retardation time $\langle \Delta t(R) \rangle$, we find:

$$\langle \Delta t(R) \rangle = \frac{\overline{\epsilon^2}}{8} \left(3 + \frac{2}{{l_0}^2} R L_f \right) \frac{R}{c_0}.$$

Although we would not expect our data to fit this expression precisely because we are considering a 3-D problem, we would expect our mean retardation time to have similar form, i.e., to have a retardation proportional to the square of the distance plus a very small component linear in propagation distance. Figure 3 plots $\log(\langle \Delta t(R) \rangle)$ vs $\log(R)$ of both the inverted Katz result and our 3-D data to confirm the similarity of form. Retardation times for our axial experiments are two orders of magnitude lower and are not plotted.

Figure 4, curves (a) and (b) show the variance (second moment) of travel times for 3-D and axial propagation, respectively. (Curves (c) and (d) will be discussed later.) The solid line represents the Chernov prediction of $\langle t'^2(R) \rangle = \theta^2 R L_f / (2 {T_0}^2 {c_0}^2)$. The travel time variance in the axial case clearly compares well with this linear function. However,

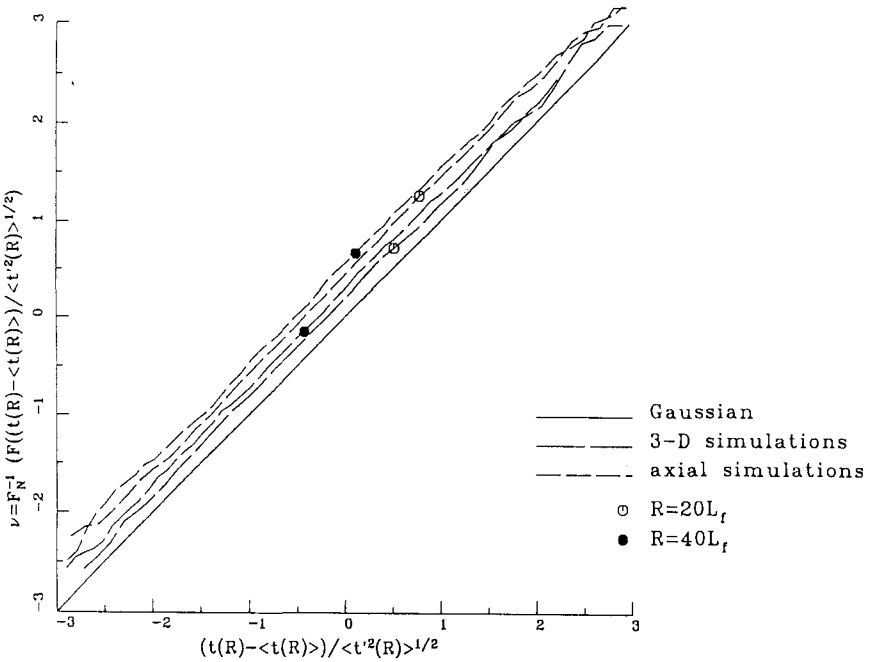

Fig. 5. Normal quantile plots of the distributions of arrival times $t(R)$ at $R = 20L$ and $40L_f$ for both axial and 3-D simulations. Data are plotted as normalized arrival times $(t(R) - \langle t(R) \rangle)/\langle t'^2(R) \rangle^{1/2}$ vs that time ν such that the cumulative distribution $F(t(R) - \langle t(R) \rangle)/\langle t'^2(R) \rangle^{1/2}$ equals $F_N(\nu)$, the cumulative distribution function of a Gaussian. Here, Gaussian distributions appear as straight lines. Curves are offset vertically for clarity.

the variance for unrestricted propagation progressively exceeds the Chernov result. An interpretation and discussion of these findings appear in Karweit *et al.*[7] and Karweit and Blanc-Benon.[10]

The normalized third moments—the skewnesses—of the travel time pdfs are essentially zero for both the axial and 3-D trajectories. The normalized fourth moments—the flatness factors—of the travel time pdfs have values within 10% of those of a Gaussian distribution, i.e., 3.0. To further suggest that these pdfs are indeed Gaussian, we plot in Fig. 5 the pdfs of arrival times for both axial and 3-D propagation at two distances $20L_f$ and $40L_f$ as normal quantile plots. In this representation, Gaussian pdfs appear as straight lines—as do our four curves. Thus the distributions shown in Fig. 2 are essentially Gaussian, differing only in their variances and mean propagation times.

As we will show in the next section, acoustic travel-time depends almost entirely on the mean celerity of the field along the path of propagation; and that mean celerity is comprised of c_0 plus a weighted sum of wave number projections in the direction of propagation. Insofar as these projections are random variables, by the central limit theorem, the distribution of mean celerities over an ensemble of fields should be Gaussian.

6. An Approximation to Axial Propagation

In this section, we want to confirm our statements in the previous paragraph, i.e., that, in these weak perturbation fields, the difference in travel time between a phase point traveling an axial trajectory a distance R and R/c_0 is accounted for almost entirely by the spatial average of the perturbation along the trajectory. To do this, we carry out an ensemble of trajectories along the x_1 axis with modified perturbation fields. This modification consists of subtracting from each field the average value of $\epsilon(x_1, 0, 0)$ between $x_1 = 0$ and $x_1 = 40L_f$. Consequently, a phase point traveling axially between $x_1 = 0$ and $x_1 = 40L_f$ will experience a perturbation field whose spatial average is precisely zero.

Over 2000 realizations, we performed this experiment and calculated the travel-time variance. The results are given in Fig. 4 curve (d). Note that the travel time variance increases with R for small R, though not at the Chernov rate. At approximately halfway the variance peaks, then decreases to (essentially) zero at $40L_f$. At any distance other than $40L_f$, the average perturbation is nonzero since we subtracted out a single value based on $40L_f$; and the further R is from $40L_f$, the larger is the average perturbation.

From these results we must conclude that variations in arrival times depend almost entirely on the distribution of nonzero-average perturbations from each of the ensemble of fields in the direction of propagation. Thus we can express the travel time of a phase point simply as the mean perturbation (up to that distance) times distance:

$$t(R) = \int_0^R \frac{dx_1}{c(x_1, 0, 0)} \approx R/c_0 - \frac{1}{2c_0} \int_0^R \frac{T'(x_1, 0, 0)}{T_0} dx_1 \,.$$

Let $T'(x_1, 0, 0) = \hat{T}(x_1, 0, 0) + \overline{T}(R)$, where $\overline{T}$ is the spatial average of the fluctuation field

over the trajectory of propagation, and $\hat{T}$ is the remaining fluctuation. Then,

$$t(R) = R/c_0 - \frac{1}{2c_0T_0}\int_0^R \hat{T}(x_1,0,0)dx_1 - \frac{1}{2c_0T_0}\int_0^R \overline{T}(R)dx_1 = R/c_0 - 0 - \frac{R\overline{T}(R)}{2c_0T_0}.$$

The spatial average of the celerity field is easy to calculate, since our perturbation fields are made up of a sum of Fourier modes. Each mode contributes separately to $\overline{T}(R)$ as

$$\overline{T}(R,k_1,k) = \frac{1}{R}\int_0^R |A(k)|\cos(k_1x_1+\phi)dx_1\,,$$

where $|A(k)|$ is the amplitude of the Fourier mode having wave number k, k_1 is the projection of wave vector $\mathbf{k}$ along x_1, and ϕ is a random phase. We can reduce this to:

$$\overline{T}(R,\,k_1,\,k) = |A(k)|B(k_1,\,R)\cos\left(\frac{k_1R}{2}+\phi\right),$$

where

$$B(k_1,\,R) = \frac{2}{k_1R}\sin\left(\frac{k_1R}{2}\right).$$

These two expressions, although integrated along x_1, are valid for any direction of propagation by considering the projection of the wave vector $\mathbf{k}$ along the axis of propagation. We will refer to the projection of $\mathbf{k}$ in the direction of propagation as k_p.

Thus, in this simplification, the variability of phase point travel time is simply a sum of cosines terms with random phases, and with amplitudes which depend on k_1 and R.

We can deduce this result directly from the energy spectrum $G(k)$. Insofar as we have restricted our ray propagation to the x_1-axis, phase points are affected only by variations along that line which are spectrally represented as the 1-D scalar power spectrum in the k_1 direction:

$$G^{(1)}(k_1) = \frac{1}{2}\int_{k_1}^{\infty}\frac{G(k)}{k}dk$$

(Ref. 18). For our $G(k)$, $G^{(1)}(k_1)$ is trivially integrated to yield $G^{(1)}(k_1) = (\theta^2 l_0/2\sqrt{\pi})\exp(-k_1^2 l_0{}^2/4)$. Here, the power is mostly contained in the low wave numbers. In fact, there is peak power at $k_1 = 0$, i.e. in the mean. (This phenomenon is not unique to a Gaussian-derived spectrum, nor to scalar fields. See, for example, Batchelor,[19] and, more recently, the wind-tunnel turbulence experiments of O'Neil and Meneveau.[20])

What this result implies is that the axial trajectories of acoustic phase points are determined by progressively lower wave number perturbation modes. And as our discrete wave number example above indicates, only those modes which have nonzero averages over the distance R have any contribution at all.

Refer again to the equation for $\overline{T}(R,\,k_1,\,k)$. $B(k_1,\,R) = 2\,\sin(k_1R/2)/(k_1R)$ is familiar to turbulence experimentalists. It expresses the so-called "length correction" for measuring velocity fluctuations with a hot wire anemometer where the received signal is just the average velocity along its length.[21] A hot wire of finite sensing length will see no contribution from a velocity perturbation whose positive and negative values along the length of the wire just

cancel, and will have varying contributions from other velocities depending on their scale of fluctuation and the length of the hot wire. This is a precise analogy to our axial propagation problem where travel time depends only on the average perturbation along its trajectory.

$B(k_1, R)$ acts as a spectral filter on $G^{(1)}(k_1)$. For very small k_1R, $B(k_1, R) = 1$, and the full spectrum of $G^{(1)}(k_1)$ contributes to the travel time variation. However, as k_1R increases, $B(k_1, R)$ begins to approach the value $1/(k_1R)$. This, in effect, filters out the perturbation contributions from larger k_1. In our case, at a distance of $40L_f$, $R = 3.54$ m. Consequently, it is only $k_1 s < 1$ that contributes significantly to the result.

This analysis applies, of course, only to axial propagation. But, the effect remains in the full 3-D propagation problem, to wit, Fig. 4 curve (c). These are the travel time variances of an ensemble of phase points which have been allowed to meander via the full ray-trace equations, but whose propagating media have had the mean value of the perturbation along the x_1-axis subtracted out for the distance $40L_f$. Whereas, for axial rays we obtained a variance of zero at $40L_f$; here, because the phase points are meandering somewhat off the axis, the value is nonzero. The more important comparison, however, is with curve (b) where unrestricted trajectories were calculated over undoctored fields. In this case, the reduction in variance at $40L_f$ is approximately 20%.

The very-low wave number dependence of acoustic propagation which has just been demonstrated suggests that simulations using "box model" fields may incur problems. That conjecture is investigated in the next section.

7. Experiments Using the Box Model

The trajectories of phase points were followed through box model simulated fields having the same Gaussian-derived fluctuation spectrum as above. Over an ensemble of 1000 realizations, phase points were followed a total distance of $40L_f$—slightly less than two box lengths—using the full 3-D ray-trace equations. The initial direction of propagation was the x_1 direction.

Unlike the random model, here we have wave vectors in predetermined directions—those specified by the 14^3 lattice. And with respect to the direction of propagation—predominantly the x_1 direction—our complete collection of Fourier modes consists of 14×14 planes of wave vectors for which their k_1 projections are $k_1 = n/(3l_0)$, where n takes on integer values from -7 to 6. Fully 14×14 of our modes contribute only in the mean to the fluctuation field, i.e., $n = 0$. The remaining modes contribute in seven discrete steps of wave number.

To understand the contributions of these modes to acoustic travel time in the x_1 direction, we ran three sets of experiments: one in which the fields consisted of only those wave vectors in the lattice whose k_1 components were zero, one in which the fields consisted of only those wave vectors whose k_1 components were nonzero, and one in which all 14^3 wave vectors were present. The results for travel-time variance are presented in Fig. 6.

Here we see that, except for very short distances of propagation, the impact of fields having fluctuations with only nonzero k_1 components is extremely small and is very sensitive to the period of the box—in this case $R/L_f = 21.3$. The impact of fields having only $k_1 = 0$

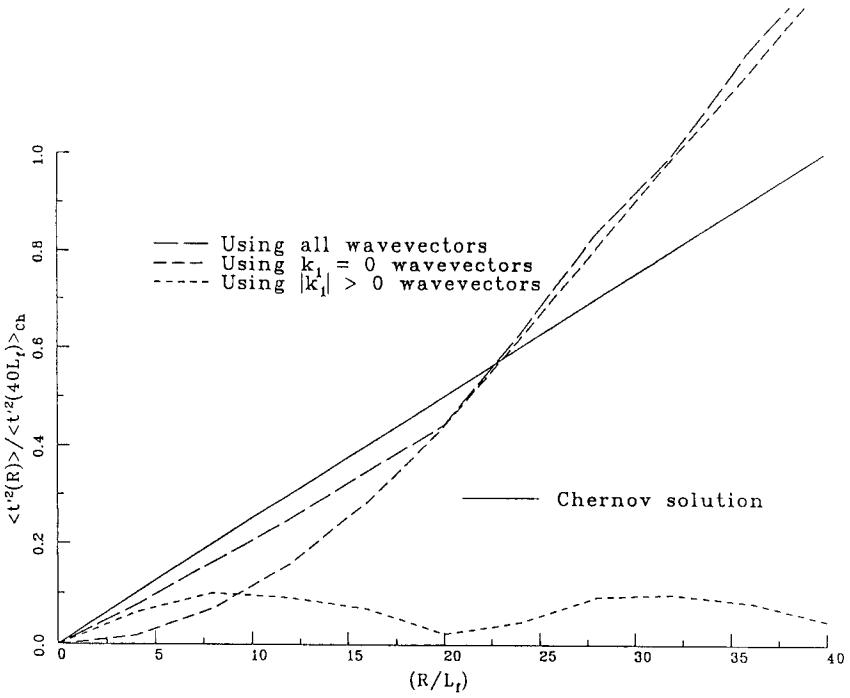

Fig. 6. Arrival time variance for rays propagating in the x_1 direction through periodic fields. Three types of fields are considered: those prescribed by a full lattice of wave vectors k_i, those prescribed by a lattice in which only wave vectors with $k_1 = 0$ are present, and those prescribed by a lattice in which only wave vectors with $|k_1| > 0$ are present. Results are accumulated over 1000 realizations and normalized with respect to the Chernov solution $\langle t'^2(R)\rangle_{Ch}$ at a distance of $40L_f$. The Chernov solution is plotted for comparison.

components is quite the reverse. In this latter case, each field presents a constant increase or decrease in celerity to a phase point along the whole trajectory. Consequently, travel times will differ from R/c_0 in proportion to distance of propagation. This will result in a travel time variance for an ensemble of fields which is quadratically increasing with distance—as demonstrated in Fig. 6. The final curve, which plots the variance from an ensemble of fields having all 14^3 modes, is essentially the sum of the two other curves. This last result is no surprise, since in the section above, we deduced that travel time variation is made up of the effects of each of the modes in the field. Note that this final curve and its predictable extension to increased distances do not compare, even qualitatively, to the Chernov result.

The experiments run for Fig. 6 are, of course, a very special case—they were run with the initial propagation in precisely the x_1 direction. That particular direction gave rise to a unique discretization of wave vector components in the direction of propagation. What results are obtained if the initial propagation is at an angle with respect to the lattice of wave vectors?

Figure 7 illustrates the effect on the projection of the latticed wave vectors when the direction of propagation is not aligned with the edge of the lattice. In this example, the direction of propagation is 2° from the x_1 direction along the diagonal. Here, each wave vector in the lattice is represented as a point whose ordinate is its wave number and whose abscissa

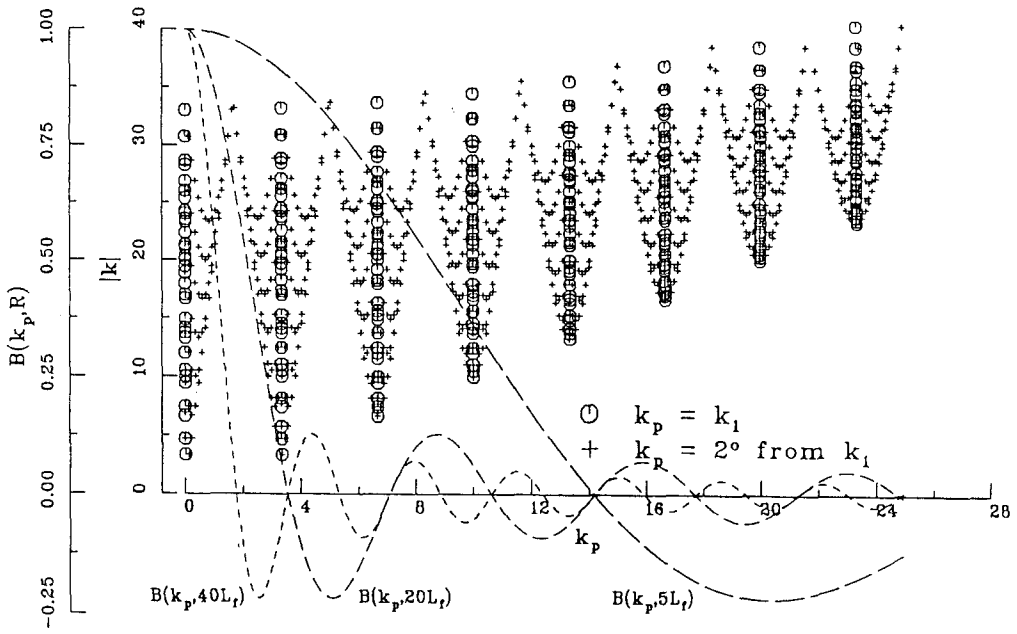

Fig. 7. Projection of wave vectors on a lattice in the direction of ray propagation. The crosses show the broadening of the wave vector components in 2-D when the angle of projection is 2^0 from the x_1 direction. The spectral filter $B(k_p, R)$ as a function of wave number k_p for several propagation distances R is superposed to illustrate the diminishing effect of higher wave numbers at larger R with respect to acoustic travel time.

is its projection in the direction of propagation k_p. The circles reflect the case previously discussed where $k_p = k_1$. Note that there are only eight discrete projections on k_1, and that wave vectors of many magnitudes contribute to similar projections.

The crosses reflect the present case. Wave vectors having identical projections in the former case are now smeared in a systematic continuum. The three superposed curves represent the low-pass spectral filter $B(k_p, R)$ for three propagation distances, $R = 5L_f, 20L_f, 40L_f$. Recall that $B(k_p, R)$ is the weighting function by which each projected Fourier mode is multiplied for its contribution to the phase point travel time. Note that, at even a distance of $R = 5L_f$, over half of the larger modes comprising the field have lost their influence. By $R = 40L_f$, only the lowest modes are important. How does propagation direction, then, impact on acoustic travel-time variance in simulated box-model fields?

Figure 8 contains the answer. Here, results are plotted for ensembles of experiments which began with a variety of different initial directions of propagation—each using fields generated from the box model. A curve generated from experiments using the random model is included for comparison. The obvious effect of the periodicity of the box is reduced when the initial angle is at least 8°. And the distance at which the periodicity is encountered increases with the cosecant of the initial angle of propagation to a maximum of $\sqrt{3}$ at 45°. But the variances are systematically low for distances within one box period and moderately scattered for distances over one box period. For the cases of 0° and 2°, higher than expected variances occurred because there was an excess of wave vectors whose projections in the

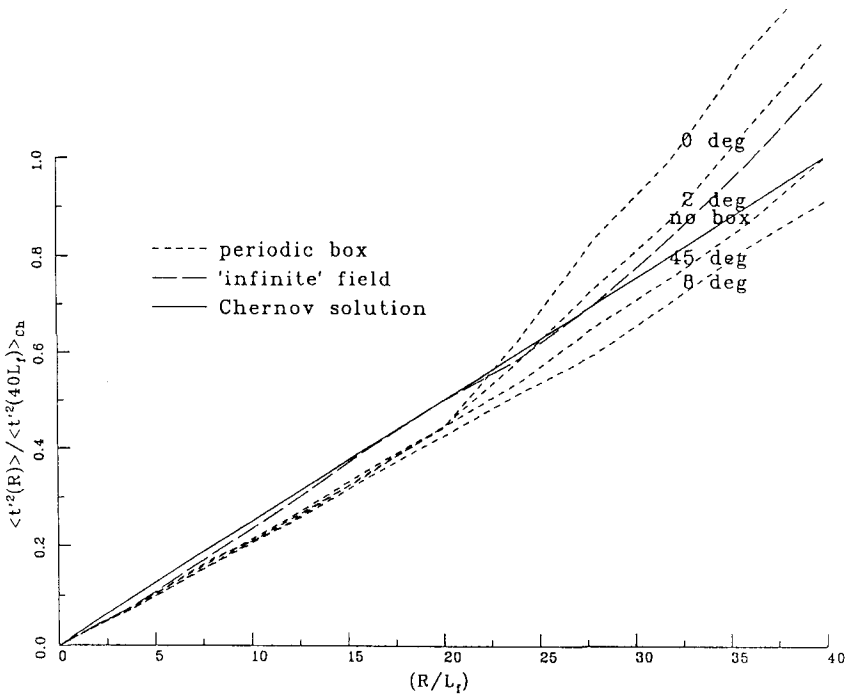

Fig. 8. A comparison of arrival-time variances for propagation through "infinite" and periodic fields. Curves are plotted for four different initial angles of propagation in the periodic fields. Results were obtained from 2000 realizations and are normalized to the Chernov calculation at a distance of $40L_f$.

direction of propagation were zero or very small. Conversely, for the cases of 8° and 45°, lower than expected variances occurred because there was a relative deficit of wave vectors whose projections were very small. Unfortunately, using the box model, the results that one obtains appear to be very geometrically dependent.

8. Conclusion

In this study, we have modeled random isotropic perturbation fields as sums of Fourier modes in two ways: with randomly oriented wave vectors (random model) and with lattice-determined wave vectors (box model). The random model was chosen originally for its ability to generate random fields of infinite extent with prescribed spectra—essentially "cheap turbulence". In the present paper, we have discovered that the most important feature of this technique is its ability to contain very low wave numbers projected along any given direction. As our axial propagation analysis showed, it is only the very lowest wave numbers that significantly contribute to variations in travel time.

Our immediate result using the random model is the description of the pdf of acoustic travel time as a function of distance traveled in weakly inhomogeneous scalar fields. That result is based on following the trajectories of acoustic phase points through an ensemble of simulated fields numerically integrating the ray-trace equations.

The more crucial result using this model is our understanding of what features of simulated inhomogeneous fields are most important for acoustic propagation.

A deficiency of the present random model, however, is the difficulty of introducing time dependency to the field, were it necessary. But, unless one could accommodate very large grids which could represent both the inner scale (high wave number) and a very long spatial periodicity (very-low wave number), the turbulence community's box models may not be the answer either. As we have seen with our box model experiments, there exist geometric artifacts associated with latticed fields which appear to strongly influence the simulation of acoustic propagation. As indicated above, the lowest modes of the 1-D power spectrum in the direction of propagation are the determinants of acoustic propagation. And in box model fields, these are the very modes that are missing. (An interesting attempt to model nonperiodic, but time-evolving, turbulence is Turfus and Hunt[22]).

Truman and Lee[23] numerically simulate the axial propagation of an optical wave through a turbulent shear layer in which the flow is prescribed by periodic boundary conditions. They present only qualitative results for travel time differences, depending on the direction of propagation. But one must wonder to what extent their results were affected by the imposed constraints of the field.

Our observations are based on latticed *scalar* fields. What the effect of periodicity and direction of propagation would be in *vector* fields requires further study. Since each Fourier mode in a vector field has an additional degree of freedom, the problems presented here might be reduced. Also, by using a larger number of lattice points (128^3 elements are now possible), an extended range of lower wave numbers could be accommodated. This would surely help considerably—but then constructing the fields would no longer be "cheap".

In summary, it would seem, that if box models were to be used for the study of acoustic propagation, the difficulties we have encountered here would, at least, have to be explicitly addressed.

References

1. L. Chernov, *Wave Propagation in a Random Medium* (McGraw-Hill, New York, 1960).
2. V. I. Tatarski, *The Effects of the Turbulent Atmosphere on Wave Propagation* (I. P. S. T. Keter Press, Jerusalem 1971).
3. J. B. Keller, "Wave propagation in random media," *Proc. Symposium Appl. Math. 13, Am. Math. Soc., Providence, RI,* (1962) 227–246.
4. E. J. Katz, "A ray theory for wave propagation in a non-uniform medium," *J. Fluid Mech.* **16** (1963) 343–356.
5. J. L. Codona, D. Creamer, S. Flatte, R. Frehlich, and F. Henyey, "Average arrival time of wave pulses through continuous random media," *Phys. Rev.* Let. **55** (1985) 9–12.
6. B. J. Uscinski, "Analytical solution of the fourth-moment equation and interpretation as a set of phase screens," *J. Opt. Soc. Am.* **2** (1985) 2077–2091.
7. M. Karweit, Ph. Blanc-Benon, D. Juvé, and G. Comte-Bellot, "Simulation of the propagation of an acoustic wave through a turbulent velocity field: A study of phase variance," *J. Acoust. Soc. Am.* **89** (1991) 52–62.
8. Ph. Blanc-Benon, D. Juvé, M. Karweit, and G. Comte-Bellot, "Numerical simulation of acoustic waves propagating through a turbulent medium," *J. d'Acoustique* **3** (1990) 1–8.

9. D. Juvé, Ph. Blanc-Benon, and G. Comte-Bellot, "Transmission of acoustic waves through mixing layers and 2-D isotropic turbulence," *Organized Structures and Turbulence in Fluid Mechanics*, ed. O. Metais and M. Lesieur (Kluwer, Boston, 1990) 367–384.
10. M. Karweit and Ph. Blanc-Benon, "Arrival-time variance for acoustic propagation in 3-D random media: the effect of lateral scales," C.R. Acad. Sci Paris, t316, Series II, (1993) 1695–1702.
11. R. S. Rogallo, "Numerical experiments in homogeneous turbulencem," NASA Tech. Memorandum 81315, (1981).
12. J. O. Hinze, *Turbulence* (McGraw-Hill, New York, 1959).
13. J. Neubert and J. Lumley, "Derivation of the stochastic Helmholtz equation for sound propagation in a turbulent field," *J. Acoust. Soc. Am.* **48** (1970) 1212–1218.
14. S. Candel, "A review of numerical methods in acoustic wave propagation," *Recent Advances in Aeroacoustics*, ed. A. Krothapalli and Ch.A. Smith (Springer Verlag, New York 1983).
15. A. D. Pierce, *Acoustics: An Introduction to Its Physical Principles and Applications* (McGraw-Hill, New York 1981).
16. B. S. White, "The stochastic caustic," SIAM J. *Appl. Math.*, **44** (1984) 122–149.
17. Ph. Blanc-Benon, D. Juvé, and G. Comte-Bellot, "Occurrence of caustics for high frequency acoustic waves propagating through turbulent fields," *Theor. and Comp. Fluid Dynamics* **2** (1991) 271–278.
18. L. S. G. Kovasznay, M. S. Uberoi, and S. Corrsin, "The transformation between one- and three-dimensional power spectra for an isotropic scalar fluctuation field," *Phys. Rev.* **76** (1949) 1263–1264.
19. G. K. Batchelor, *The Theory of Homogeneous Turbulence* (Cambridge 1960).
20. J. O'Neil and C. Meneveau, "Spatial correlations in turbulence: Predictions from the multifractal formalism and comparison with experiments," *Phys. Fluids* **A5** (1993) 158–172.
21. M. S. Uberoi and L. S. G. Kovasznay, "Influence of resolving power on measurement of correlations and spectra of random fields," Project Squid, Ofc. of Naval Res. and Ofc of Air Res., tech. report 20 (1951).
22. C. Turfus and J. C. R. Hunt, "A stochastic analysis of the displacements of fluid elements in inhomogeneous turbulence using Kraichnan"s method of random modes," *Advances in Turbulence*, ed. G. Comte-Bellot and J. Mathieu (Springer Verlag, Berlin, 1987) 191–203.
23. C. R. Truman and M. J. Lee, "Effects of organized turbulence structures on the phase distortion in a coherent optical beam propagating through a turbulent shear flow," *Phys. Fluids* **A2** (1990) 851–857.